Quantifying Performance Benefit of Adaptive Active-Passive Mode-Switching Using Experimental Data.

Jacob Fromage[1], Rikki Masson[1], Piers J. Beasley[1], Matthew A. Ritchie[1], Kevin Chetty[2]
[1]*Department of Electronic and Electrical Engineering*
[2]*Department of Security and Crime Science*
University College London, London, United Kingdom
{jacob.fromage.23}{rikki.masson.23}{piers.beasley.19}{m.ritchie}{k.chetty}@ucl.ac.uk

***Abstract*—In this paper we investigate the potential benefits of implementing an adaptive active-passive mode-switching algorithm to a multi-function radio frequency (RF) system for sensing. This research was performed using experimental radar data captured during a trial of a hybrid active-passive capable software defined radio (SDR) based radar. An outline of the system used during the experiment is included within the paper, as well as an overview of the experiment itself. Details of the post-processing performed on the data and results produced from running the algorithm on the experimental data are shown. The performance benefits of a real-time application of the algorithm are quantified and verified in the form of figures and tables. In some cases a 60% reduction in active transmission time is realised, as well as a 20% increase in mean SNR over time when compared with data not implementing the algorithm. The strengths and limitations of the algorithm in its current form are discussed as well as directions for future work.**

Keywords—Hybrid Radar, Multifunction, Multi-function, Passive Radar, Sensor Fusion, Adaptive Signal Processing, Software Defined Radio, Experimental data

I. INTRODUCTION

In recent years, there has been an increase in desire for flexible multi-function/multi-role radio frequency (RF) systems for sensing. It is now the case that hardware capabilities are beginning to be able to match these desires. Both theorised and realised applications of these systems include hybrid synthetic aperture radar (SAR) systems [1], multistatic active and passive sensing systems [2], airborne systems and more recently through-the-wall sensing applications for policing and disaster relief [3].

Discussions around multifunction sensors with regards to electronic warfare (EW) are also beginning to surface [4]. The agility afforded to these sensors due to their multi-functional nature makes countermeasures an active area of research. In recent years, consumer-off-the-shelf (COTS) software defined radios (SDRs) have grown in popularity tremendously as a result improvements in hardware capabilities. Many of these solutions offer a very good price to performance ratio making them attractive options for researchers [5]. Exploiting the multi-mode capabilities of these devices for increased detection performance in different bands has been demonstrated before [6] [7], but real-time mode-switching and adaptability is not an area that has been investigated in prior publications.

This paper focusses on hybrid active-passive radar functionality using experimental radar data. The capacity to utilise both types of sensing allows a multifunction system to operate in the optimum mode for a given scenario based on the strengths and weaknesses of both active and passive sensing.

Passive radar has many advantages over active radar. One such advantage is that without an active transmission, the likelihood of the passive radar system being detected by Electronic Surveillance (ES) methods becomes much smaller. A potential exploitation of this would be to locate a target using a passive sensing configuration, a passive detection would then cue the active radar to sense in the direction of the detection. This in turn would reduce the overall RF emissions in other directions, lowering the probability of interception by ES systems in the area.

Another advantage of a passive system is lower size, weight and power (SWaP) requirements. A passive system does not require its own dedicated transmitter, and therefore also does not have any transmitter related power cost. This benefit can be capitalised on further by the passive receiver being able to continuously receive whilst maintaining a low power cost. The long receive times permit long integration times which can give very high Doppler resolutions and can increase target sensitivity through coherent integration gain.

A key drawback is by nature passive radar requires an illuminator of opportunity (IoO) of suitable power in order to sense effectively. A further drawback is that many IoO's such as digital video broadcasting towers and satellites have waveforms designed for communication and therefore lack optimisation for sensing [8]. Furthermore, beamsteering on transmit cannot be achieved as the passive radar operator is not in control of the IoO. The advantages of active radar are antonymous to the weaknesses of passive radar, and hence contribute to the reason hybrid radar systems are becoming a more and more popular topic of research.

The driving idea behind the research presented in this paper is that a radar system that could automatically switch modes in real time based on parameters set by the operator would be incredibly powerful. There are many scenarios where the cost of transmission may be very high and so passive radar is favourable. However, passive radar is not always an option. For example, on a moving airborne platform there may be occasional periods where the signal from the IoO is not providing sufficient signal-to-noise ratio (SNR) for the passive radar to function optimally. This could be due to the distance away from the IoO or the bistatic angle and geometry being undesirable and providing SNR too low for detection. In a situation passive radar becomes unusable, a form of active transmission may be required. If this can be performed on the

same system and automated to a required specification, the systems SWaP parameters will be reduced. Additionally, both operator workload and cost of the overall system will be reduced.

Earlier work by Beasley et al. [9] indicated that adaptability in a hybrid system is important due to the variable detection performance that may be encountered in real-world scenarios. One factor that can affect passive radar performance is evolving bistatic geometries as a platform moves through space. This paper is intended to be a first exploration into the implementation of adaptability in a hybrid sensing system. Specifically, in the form of active/passive mode switching based on defined parameters applied to experimental data.

II. System and Experimental Method

This section will briefly describe the hybrid system used to obtain the experimental data as well as outline the experiment that generated the data used in this research.

A. Hardware Solution

The radar system used for the experiment that generated the data set used in this paper is named bladeRAD [10]. BladeRAD is multistatic enabled radar system capable of both active and passive modes developed by Beasley [10]. The system is based on the Nuand bladeRF micro 2.0 xA4 SDR. This is a low cost and highly configurable SDR available for approximately $540 USD. The bladeRF xA4 has a central frequency limit of 6 GHz, with channel bandwidths that can be programmed between 0.2 MHz to 56 MHz. It uses the AD9361 transceiver RFIC which is capable of 2 X 2 MIMO. P J Beasley adapted several of these SDRs to create bladeRAD. For use as a monostatic radar transceiver Beasley split the TX and RX streams across two separate SDRs that are then connected to the same PC. In this configuration a 40 MHz transceiver bandwidth was measured [10]. In order to achieve hybrid sensing, a third bladeRF SDR is added to the above configuration in a purely passive mode.

The data featured in this paper was captured using the FMCW mode of the radar. All signal processing was performed post capture in MATLAB®. Deramping of the Rx channel is performed post-capture using a prerecorded FMCW chirp as shown in Fig. 1. Fig. 2 shows the passive workflow.

For an in-depth description of the bladeRAD system and its performance metrics, please see [10].

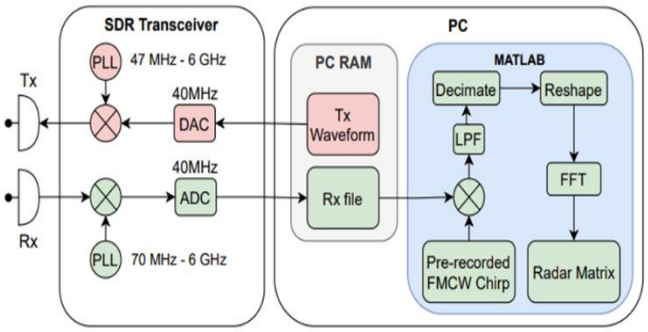

Fig. 1. Simplified signal processing flow of bladeRF based monostatic FMCW radar transceiver. (Figure taken directly from [10].)

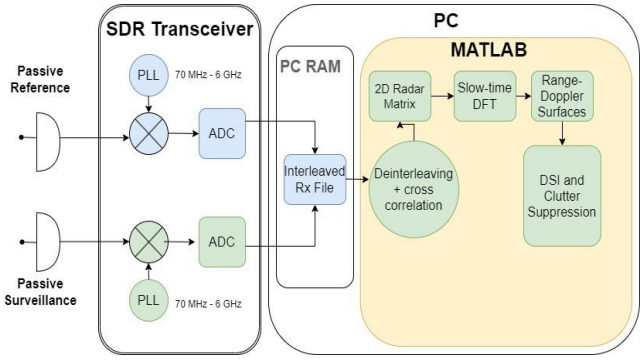

Fig. 2. Simplified processing flow of passive mode SDR

B. Experimental Scenario

The data used in this paper was obtained from the experiment described in [9]. The IoO for the passive sensing was DVB-T tower with a central RF of 0.69 GHz, a bandwidth of 7.61 MHz and a Tx power of 170 kW. The IoO was 8.70 km to the southeast from the sensing passive bistatic radar (PBR). Fig. 3 is a visual representation of the experimental setup, it also shows the direction of target motion relative to the hybrid radar system. The experiment used two targets, however, the data used in this paper is the data obtained from capturing the movement of the second target, a small two-door Renault Clio car [9]. The bistatic angle, $\beta = 0°$ to allow for direct comparison of the active and passive data streams.

III. Post-Processing

In this section, the process for converting the resulting data of the initial experiment into the form that was required for this research will be described. The results from the initial experiment showed that the movement of the car towards the hybrid system was clearly detectable across both sensing types [9]. The SNR increases as the slice number, and hence time, increases due to the target moving towards the radar during the experiment.

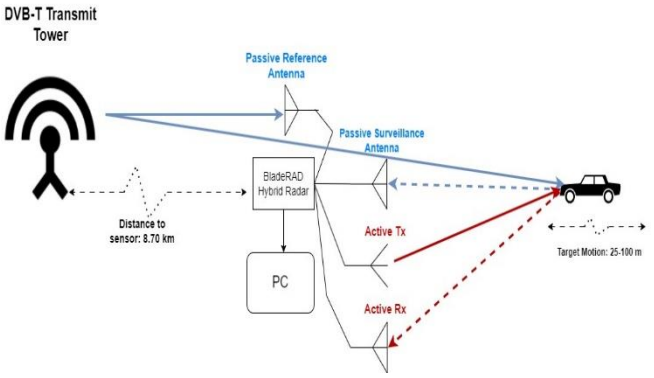

Fig. 3. A diagram of the bladeRAD hybrid radar experimental setup, from which the data used in this paper was obtained.

A. Processing the Results

Initially, the data was in the form of active and passive range-doppler surfaces. In order to compare the active and passive radar SNR over the evolution of slices, it was necessary to extract both the peak signal magnitude as well as the mean noise of each slice. a function was developed in MATLAB® to extract these parameters. The function operated on the IQ data of the range-doppler slices. Both the active and passive data streams were comprised of 145 individual range-Doppler slices. The function first calculates the absolute value of each component of the 2D matrix, IQ_{abs}. Next, the function converts the absolute values to their values in dB, IQ_{dB}.

$$IQ_{dB} = 20\log_{10}(IQ_{abs}) \quad (1)$$

The function then finds the largest value of IQ_{dB} and defines this as the signal. In Fig. 4 it can be observed that in the first 10 m the direct signal breakthrough between Tx and Rx antennas is of similar magnitude to the target backscatter. This was present in all active slices. To mitigate this, a form of masking was implemented on the first 5 range bins when calculating the peak return. This equates to the first 20 m of the range-Doppler surface being excluded from the calculation.

The function also included a mean noise value calculation. To ensure the mean noise value was unaffected by the large signal returns from the target as well as the close-range spikes, a configurable region of the range-Doppler slice is selected, and the mean of the region is calculated and defined as the noise. It is important to note that the mean of the region is calculated after the absolute values have been calculated and converted to the dB scale. With a value for the signal and a value for the noise defined, the function calculates the SNR for the slice.

$$SNR = Signal_{dB} — Noise_{dB} \quad (2)$$

As can be observed in Fig. 6, for both active and passive data streams, the calculated SNR is very high across all slices.

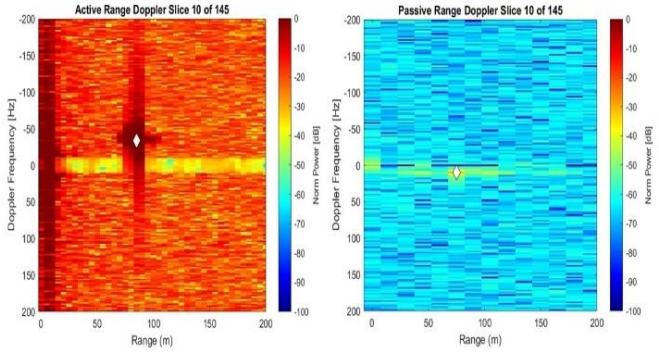

Fig. 4. An example of one of the 145 range-Doppler slices for active data (left) and passive data (right). White diamond indicates peak signal return.

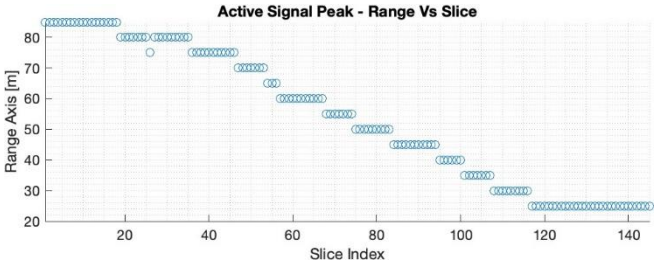

Fig. 5a. The blue dots show the range in meters for the peak target backscatter. This figure is for active data.

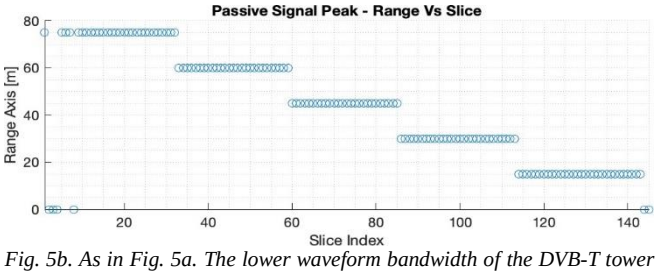

Fig. 5b. As in Fig. 5a. The lower waveform bandwidth of the DVB-T tower meant a lower ADC rate and as such the range bin size is lower for the passive data set.

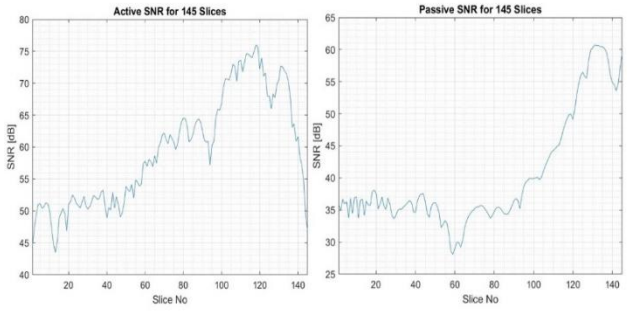

Fig. 6. SNR against Slice for Active range-Doppler slices (left) and Passive range-Doppler slices (right).

B. Degrading the data

The SNR shown is from real experimental data, it is a good representation of what can be expected from this hybrid system in ideal conditions. An IoO with 170 kW Tx power and full line-of-sight will not always be possible in a real-world scenario. In order to have the data represent a more realistic scenario of a hybrid system, both active and passive data streams were degraded. To degrade the SNR of each data stream, bespoke noise matrices were added to the original

range-Doppler surfaces. The noisy matrices were calculated in such a way that a desired mean SNR for the data is input, this input is then acknowledged in the calculation of the randomised noise matrix to ensure the random numbers are capped. Following the combination of the original IQ data and the noise matrix, the new noise infused data is then processed by the function described in II.A to give new SNR values for every slice.

IV. Mode-Switching Algorithm

This section will discuss the decisions made in reference to the mode-switching algorithm, the justification for the thresholding and the results obtained from different noise levels.

A. Thresholding

When the active and passive noise infused SNR against slice graphs are plotted on the same axis, many points of intersection can be observed. When visualised in this way, it becomes clear where switching between modes would result in an increase in SNR. However, there are many circumstances in which passive sensing is preferable to active sensing. For this reason, when designing the mode switching algorithm, maximising SNR was not selected as the determining factor. Instead, passive mode was set as the preferred mode, unless the passive SNR fell below the determined threshold. When the SNR is below the selected threshold, the algorithm will select the mode with the highest SNR. Example A of this decision-making process is visualised in Fig. 7. Here, the SNR of the active and passive data streams have been degraded by a mean of 50 dB and 30 dB respectively and the threshold SNR has been set to 10 dB. A for loop was established to act as a counter for the number of slices the algorithm chose each mode. Results relating to example A are shown in Table 1. In this case, the hybrid system would have only been active 33.9% of the time. If operating covertly, this would be highly desirable as minimising radiation is crucial to remaining undetected to any ES systems that may be operating in the area of operation. Furthermore, this is a 2/3 reduction in Tx power consumption. Setting the threshold to 5 dB in this case results in an even greater utilisation of passive mode of 82.07%. The desired SNR threshold can be changed to meet the requirements of the scenario and trade-offs can be evaluated by the user.

In Fig. 7, it can be observed that between slice 100 and ~ slice 125 the algorithm is selecting the passive mode despite a large decrease in SNR between the two modes. This is intentional as, for the purposes of this paper, the prioritisation for the mode-switching algorithm was to remain in a passive sensing mode for as long as possible based on a given SNR threshold. There is scope for investigation into how much of an SNR decrease is acceptable to remain in a passive sensing mode. A more complex algorithm that is based on many different factors is a goal for future work.

Example B of the algorithm in-use is displayed in Fig. 8. Here, the signals are degraded in such a way that the SNR for each slice in both data streams oscillates randomly around 0 dB. This was achieved via the method described in III.B. These data sets simulate a highly noisy environment and is an example of an extreme case. It can be observed in Fig. 8 that switches must occur rapidly between slices to remain above the defined threshold of 0 dB. Table 2 shows the counter data for Fig. 8. This more frequent switching may be computationally challenging for a given system, and so modifications may need to be made to the decision-making algorithm to allow for a given number of slices to fall below the threshold before mode switching is engaged. Currently the thresholding is only based on a desired SNR, however this is just one method. The mode-switching algorithm could also be informed by other quantitative means such as a desired probability of detection.

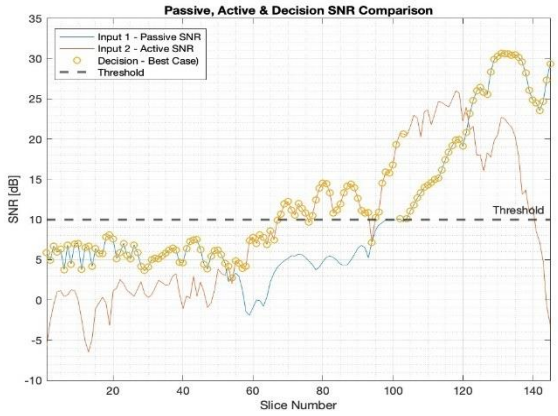

Fig. 7. A visualisation of example A of the decision-making algorithm in use. . Each yellow circle represents a slice and the plot it falls on represents the mode the algorithm has selected.

TABLE 1: Numerical results of the decision-making displayed in Fig. 8

	Number of Slices in Mode	*% of Slices*
Passive	*96*	*66.21*
Active	*49*	*33.79*

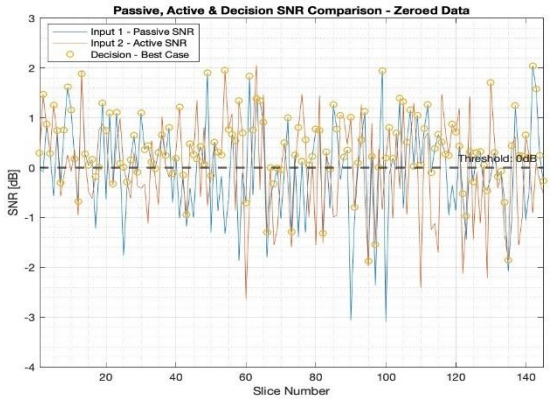

Fig. 8. A visualization of example B of the decision-making algorithm in use. Each yellow circle represents a slice and the plot it falls on represents the mode the algorithm has selected.

Table 2: Numerical results of the decision-making displayed in Fig. 9

	Number of Slices in Mode	*% Percentage of Slices*
Passive	*90*	*62.07*
Active	*55*	*37.93*

B. *Average SNR Improvements*

A promising result common to both examples of the mode-switching algorithm in use is an increase in mean SNR across all slices. Fig. 9 and Fig. 10 show that the minimum SNR against slice is increased in both cases. This further demonstrates the advantages of an adaptive hybrid radar. In many cases, receiver operating characteristic (ROC) curves are used to plot probability of detection (Pd) as a function of SNR and probability of false alarm (Pfa). It follows that an increase in mean SNR across slices would also lead to an increase of Pd across all slices on such a curve. There may be some real-world scenarios where maximising Pd is essential. In these cases, the algorithm could be altered to choose the mode reporting the highest SNR. This would ensure the highest Pd was achieved for a given slice. This is an area being considered for future work.

Fig. 10 shows that the maximum SNR when the algorithm has been run on the data is lower than the active stream alone. This is due to the passive mode preference inherent to the thresholding. Provided a passive slice reports an SNR ≥ the threshold, passive mode will be selected. This takes place regardless of the magnitude of difference in SNR between active and passive slices. This can be altered by the user to align better with the use-case.

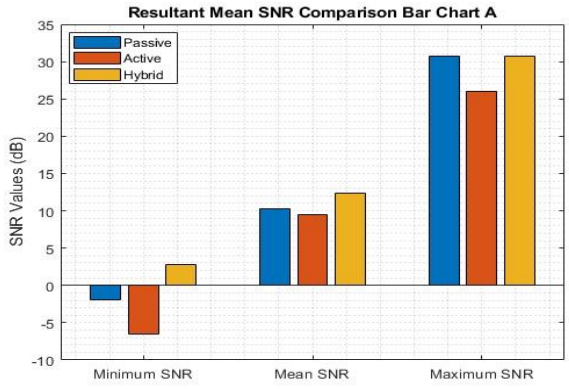

Fig. 9. A bar chart showing useful comparisons of SNR values before and after the data is passed to the algorithm. Corresponds with example A. Hybrid = algorithm results.

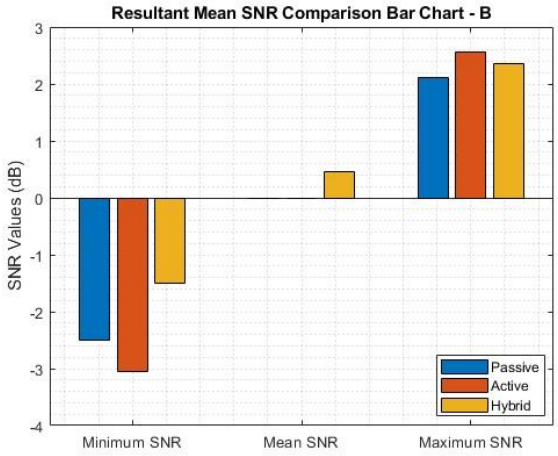

Fig. 10. A bar chart showing useful comparisons of SNR values before and after the data is passed to the algorithm. Corresponds with example B. Hybrid = algorithm results.

V. Conclusion

Within this work we have introduced the concept of a real-time mode-switching hybrid radar. Previous experimentation has shown bladeRAD [10] to be capable of both active and passive sensing of a moving target. Coupled with the development of the MATLAB® functions that are described in III, it has been demonstrated that mode-switching would provide measurable benefits to a hybrid system in a multitude of circumstances that are relevant to real-world hybrid radar applications.

Areas for future work have been identified within the text. Some examples may include jamming type data manipulation on the active channels, some tweaking of the switching parameters to reduce frequency of mode-switching and potential implementation of track-informed decision making.

It is likely any future experimental work will be undertaken using the UCL ARESTOR system [11] [12]. The increased capability of the ARESTOR multi-function RF-system-on-a-chip will open the possibility for real-time mode switching experimentation, as a considerable amount of the signal processing can be completed in real-time on the device's FPGA; allowing each modes performance to be evaluated during capture rather than offline in software post-processing, as with the bladeRAD system.

Acknowledgments

The authors would like to acknowledge EPSRC and Leonardo UK who are both providing sponsorship for this ICASE award PhD into multifunction radar systems.

References

[1] A. G. Huizing *et al.*, "Compact scalable multifunction RF payload for UAVs with FMCW radar and ESM functionality," in *2009 International Radar Conference "Surveillance for a Safer World" (RADAR 2009)*, Oct. 2009, pp. 1–6. Accessed: Feb. 19, 2024. [Online]. Available: https://ieeexplore.ieee.org/document/5438484

[2] H. Kuschel, J. Heckenbach, and J. Schell, "Deployable multiband passive/active radar for air defense (DMPAR)," *IEEE Aerosp. Electron. Syst. Mag.*, vol. 28, no. 9, pp. 37–45, Sep. 2013, doi: 10.1109/MAES.2013.6617097.

[3] J. J. M. de Wit, W. L. van Rossum, R. J. Miller, and L. Hyde, "Multifunction radar concept for through-wall surveillance," in *2013 IEEE Radar Conference (RadarCon13)*, Apr. 2013, pp. 1–6. doi: 10.1109/RADAR.2013.6586122.

[4] C. Wasserzier, J. G. Worms, and D. W. O'Hagan, "How Noise Radar Technology Brings Together Active Sensing and Modern Electronic Warfare Techniques in a Combined Sensor Concept," in *2019 Sensor Signal Processing for Defence Conference (SSPD)*, May 2019, pp. 1–5. doi: 10.1109/SSPD.2019.8751657.

[5] R. Fagan, F. C. Robey, and L. Miller, "Phased array radar cost reduction through the use of commercial RF systems on a chip," in *2018 IEEE Radar Conference (RadarConf18)*, Apr. 2018, pp. 0935–0939. doi: 10.1109/RADAR.2018.8378686.

[6] Y.-K. Kwag, J.-S. Jung, I.-S. Woo, and M.-S. Park, "Multi-band multi-mode SDR radar platform," in *2015 IEEE 5th Asia-Pacific Conference on Synthetic Aperture Radar (APSAR)*, Sep. 2015, pp. 46–49. doi: 10.1109/APSAR.2015.7306151.

[7] "Multi-mode SDR radar platform for small air-vehicle Drone detection | IEEE Conference Publication | IEEE Xplore." Accessed: Feb. 19, 2024. [Online]. Available: https://ieeexplore.ieee.org/document/8059254

[8] "Joint Waveform and Receiver Design for Co-Channel Hybrid Active-Passive Sensing With Timing Uncertainty | IEEE Journals & Magazine | IEEE Xplore." Accessed: Feb. 09, 2024. [Online]. Available: https://ieeexplore.ieee.org/document/8950300

[9] P. J. Beasley and M. A. Ritchie, “Multi-Band Hybrid Active-Passive Radar Sensor Fusion,” in *2023 IEEE Radar Conference (RadarConf23)*, May 2023, pp. 1–6. doi: 10.1109/RadarConf2351548.2023.10149774.

[10] P. J. Beasley and M. A. Ritchie, “bladeRAD: Development of an Active and Passive, Multistatic Enabled, Radar System,” in *2021 18th European Radar Conference (EuRAD)*, Apr. 2022, pp. 98–101. doi: 10.23919/EuRAD50154.2022.9784498.

[11] N. Peters, C. Horne, and M. A. Ritchie, “ARESTOR: A Multi-role RF Sensor based on the Xilinx RFSoC,” in *2021 18th European Radar Conference (EuRAD)*, Apr. 2022, pp. 102–105. doi: 10.23919/EuRAD50154.2022.9784466.

[12] M. Ritchie, N. Peters, and C. Horne, “Joint Active Passive Sensing using a Radio Frequency System-on-a-Chip based sensor,” in *2022 23rd International Radar Symposium (IRS)*, Sep. 2022, pp. 130–135. doi: 10.23919/IRS54158.2022.9905049.